

Continuous microfluidic immunomagnetic cell separation

David W. Inglis^{a)}

Princeton Institute for the Science and Technology of Materials (PRISM), Department of Electrical Engineering, Princeton University, Princeton, New Jersey 08544

R. Riehn and R. H. Austin

Department of Physics, Princeton University, Princeton, New Jersey 08544

J. C. Sturm

Princeton Institute for the Science and Technology of Materials (PRISM), Department of Electrical Engineering, Princeton University, Princeton, New Jersey 08544

(Received 4 August 2004; accepted 20 September 2004)

We present a continuous-flow microfluidic device that enables cell by cell separation of cells selectively tagged with magnetic nanoparticles. The cells flow over an array of microfabricated magnetic stripes, which create a series of high magnetic field gradients that trap the magnetically labeled cells and alter their flow direction. The process was observed in real time using a low power microscope. The device has been demonstrated by the separation of leukocytes from whole human blood. © 2004 American Institute of Physics. [DOI: 10.1063/1.1823015]

Immunomagnetic cell separation, in which magnetic particles are selectively attached to cells, has become a common technique for biological cell isolations. Typically dextran beads impregnated with iron oxide (Fe_2O_3) and coated with antibodies are bound to a particular antibody receptor on the surface of a cell. In previous work, cells are either trapped on ferromagnetic fibers which induce locally high magnetic field gradients from a relatively uniform externally applied field and then washed out after the field is removed, or are deflected in a continuous flow by an externally applied gradient of magnetic field in a macroscopic device.¹⁻⁵ In this letter, we present a magnetic cell separator that has two distinct advantages over current methods. First, it is planar and capable of being integrated with other components into a microfluidic total analysis system (μTAS). Further, because it is operating with continuous flow it can separate a large range of volumes without modification. The magnetic field gradients are created by micropatterns of a magnetic material. We also present a numerical analysis of the forces on cells labeled with superparamagnetic beads in such a device, and demonstrate the selective cell by cell separation of leukocytes from blood.

In our device, cells flow over a region of integrated microfabricated ferromagnetic stripes [Fig. 1(a)]. The magnetic field pattern from each stripe creates a magnetic trap that alters the movement of only those cells coated with superparamagnetic beads. Cells with sufficient quantity of beads become trapped over the magnetic stripes and flow only along the stripe direction, not parallel to the fluid flow (Fig. 2). Quantitatively the magnetic force \mathbf{F}_M on a particle with a magnetic dipole \mathbf{m} in a magnetic field \mathbf{H} is

$$\mathbf{F}_M = \mu_0 \nabla (\mathbf{m} \cdot \mathbf{H}). \quad (1)$$

The beads used in our case are superparamagnetic, leading to a saturation of the magnetization at relatively low magnetic fields of 0.02 T, and negligible remanence. Thus \mathbf{m} , for fields greater than 0.02 T, can be treated as a vector quantity

of constant magnitude, but parallel to \mathbf{H} , and the force becomes

$$\mathbf{F}_M = S \mu_0 \mu_B \nabla H, \quad (2)$$

where S is the number of bohr magnetons μ_B per bead and H is the magnitude of the magnetic field. The magnetically labeled cell is subject to both a force \mathbf{F}_{Mz} in the vertical direction [z as defined in Fig. 1(a)] and a force $\mathbf{F}_{M\perp}$ which acts in the plane of the device [x as defined in Fig. 1(a)]. This in plane force, $\mathbf{F}_{M\perp}$ in Fig. 2., will be perpendicular to the stripe. \mathbf{F}_{Mz} pulls the magnetic bead towards the substrate while $\mathbf{F}_{M\perp}$ acts to trap the cell in the area above the stripe. The force on a whole cell can be found by integrating the contributions of all magnetic beads on it.

For low Reynolds-number flow, the velocity \mathbf{v} of a tagged cell in the plane of the device for a magnetically labeled object with viscous drag factor ξ in a flow with bulk flow velocity \mathbf{v}_{flow} is $\mathbf{v} = \mathbf{v}_{\text{flow}} + \mathbf{F}_M / \xi$. We can identify $\xi \mathbf{v}_{\text{flow}}$ with a drag force \mathbf{F}_D . If the component of the drag force perpendicular to the magnetic stripes $\mathbf{F}_{D\perp}$ becomes less than the maximum of the magnetic force $\mathbf{F}_{M\perp}$ (Fig. 2), then the cell will be trapped above the stripe because the drag force is not sufficient to push the particle past the stripe. When this happens, the vector component of the drag parallel to the stripe will push the cell along the stripe and it will flow at an angle θ compared to the unlabeled particles. For stripes aligned at an angle θ to the fluid flow the condition for trapping can be expressed as

$$\xi \mathbf{v}_{\text{flow}} \sin(\theta) < \mathbf{F}_{\text{max}}^{\text{M}\perp}. \quad (3)$$

The magnetic field gradient needed for trapping at a given bulk flow velocity becomes progressively smaller as θ approaches 0° , but the net displacement then also approaches 0. On the other hand, for θ approaching 90° the displacement becomes infinite but the magnetic force $\mathbf{F}_{\text{max}}^{\text{M}\perp}$ has to fully balance $\xi \mathbf{v}_{\text{flow}}$. (Note that even if Eq. (3) is not fulfilled, cells are slightly deflected as they travel over the stripe, but by an order of magnitude less than if they are trapped. A complete solution of the problem will be given elsewhere.)

^{a)} Author to whom correspondence should be addressed; electronic mail: dinglis@princeton.edu

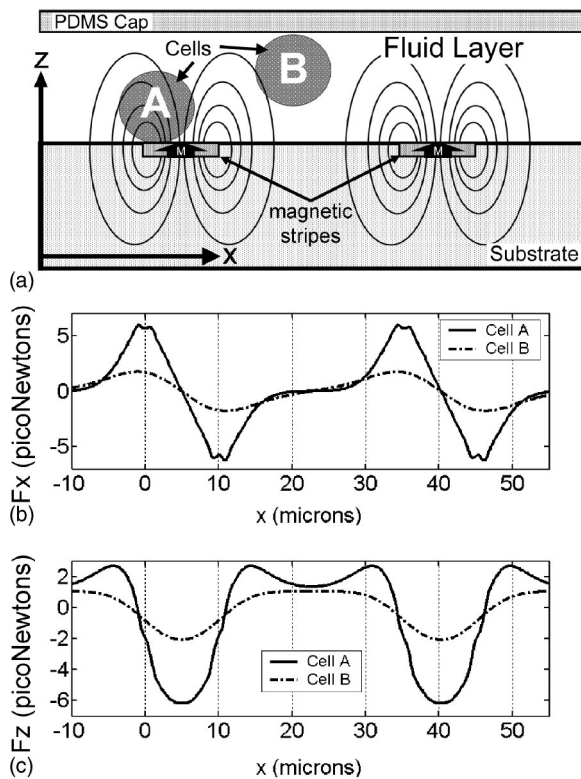


FIG. 1. (a) Cross section of the magnetic separation device showing qualitative field lines from magnetized nickel structures embedded into a silicon substrate. For simulations, the nickel is $2\ \mu\text{m}$ thick, $10\ \mu\text{m}$ wide at period of $35\ \mu\text{m}$. (b) Calculated force in the x (lateral) direction on $10\text{-}\mu\text{m}$ -diam cells A (touching surface) and B (center is $10\ \mu\text{m}$ above surface). Nickel magnetization $M=0.08\ \text{T}$, external field of $H=0.08\ \text{T}$, beads of dipole moment $m=1.8\times 10^5\ \mu_B$ and $N=5000$ beads per cell was assumed. (c) Calculated force in the z (vertical) direction on cells A and B. The net force per period is negative for both cells.

The magnetic force on a cell in the lateral and vertical directions was modeled assuming $10\text{-}\mu\text{m}$ -wide, $2\text{-}\mu\text{m}$ -thick nickel stripes at a period of $35\ \mu\text{m}$ with a uniform out-of-plane magnetization $M=0.08\ \text{T}$, and a uniform external field of $0.08\ \text{T}$. The nickel magnetization was chosen to be set at this level because it was measured experimentally in our structures with an applied field of $0.08\ \text{T}$ (in a superconducting quantum interference device magnetometer). We assumed spherical cells with a diameter of $10\ \mu\text{m}$, each labeled with 5000 beads each of $1.8\times 10^5\ \mu_B$ distributed evenly over the surface. The magnetic moment \mathbf{m} was estimated by assuming that each microbead is $50\ \text{nm}$ in diameter, 60% by weight iron oxide and 40% by weight dextran,² and $2.2\ \mu_B$ per iron atom.

Figures 1(b) and 1(c) show the vertical and horizontal (perpendicular to the stripes) components of the magnetic force on two cells. Cell A is in contact with the magnetic features, while the center of cell B is $10\ \mu\text{m}$ above the wires. The cells are attracted to the center of each magnetic stripe with maximum downward force of $6.2\ \text{pN}$, and maximum force in the x direction of $6.0\ \text{pN}$. For comparison the drag force on a $10\ \mu\text{m}$ sphere in a flow of $100\ \mu\text{m/s}$ using Stokes formula, is $9.5\ \text{pN}$.

The device consists of a silicon substrate containing recessed magnetic stripes. To fabricate the magnetic stripes, $10\text{-}\mu\text{m}$ -wide channels were etched at a period of $35\ \mu\text{m}$ into a silicon substrate and then sputter coated with nickel. The wafer was then chemically mechanically polished to achieve

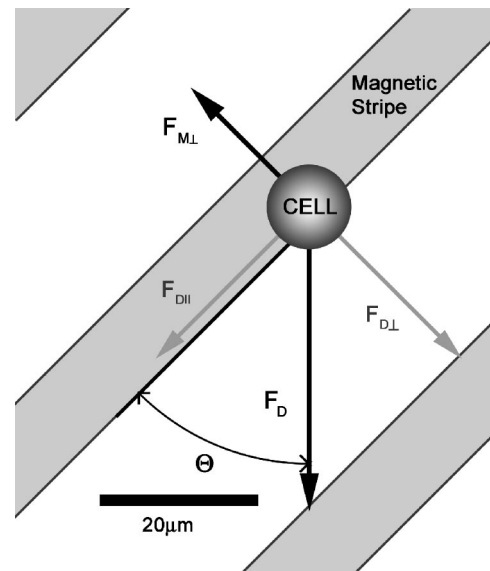


FIG. 2. Top view diagram of a magnetically labeled cell over a magnetic stripe magnetized out of plane showing in plane magnetic force $F_{M\perp}$ and fluid drag force F_D due to fluid flow at angle Θ to stripe direction. F_D is decomposed into components $F_{D\perp}$ and $F_{D\parallel}$ perpendicular and parallel to stripe, respectively.

a smooth surface with recessed nickel stripes, $2\ \mu\text{m}$ thick, with their surfaces planar with the silicon surface [Fig. 1(a)]. A $75\ \text{nm}$ silicon dioxide layer was then deposited on the wafer surface by plasma-enhanced chemical vapor deposition. A polydimethylsiloxane layer containing $15\text{-}\mu\text{m}$ -deep microfluidic channels was then sealed to the substrate to direct the flow of cells. A uniform flow of fluid in one direction (at an angle θ to the stripes) was imposed over the substrate by positive pressure combined with a row of microfluidic resistors at the top and bottom of the substrate.⁶ The cells were injected through a $40\text{-}\mu\text{m}$ -wide aperture in the middle of the microfluidic resistors. An external field H of up to $0.1\ \text{T}$ was applied using a NbFeB magnet of dimensions $2.5\ \text{cm}$ diameter by $1.9\ \text{cm}$.

To demonstrate operation of the device we labeled cells with CD45 Microbeads from Miltenyi Biotech (Auburn, CA). The beads are $20\text{--}100\ \text{nm}$ in diameter and were estimated in the previous calculations to have an average magnetic moment of $1.8\times 10^5\ \mu_B$. The CD45 antigen is expressed to varying degrees on all leukocytes. Whole, undiluted human blood less than $24\ \text{h}$ old was incubated in a heparin-coated container with a vital nucleic stain, Hoechst 33342 (Hoechst, Frankfurt, Germany) at $100\ \mu\text{g/ml}$, for $15\ \text{min}$ at $37\ ^\circ\text{C}$, and then incubated with the microbeads for $15\ \text{min}$ at $9\ ^\circ\text{C}$. After this preparation we expect all leukocytes to fluoresce when illuminated with $488\ \text{nm}$ light, and to be coated with at least 4000 beads.^{7,8} To reduce adhesion of the cells to the walls of the device, the device was soaked in a $2\ \mu\text{g/ml}$ solution of Pluronic F108 (BASF, Mount Olive, NJ) and water for at least $1\ \text{h}$.⁹ During operation, phosphate buffered saline containing $2\ \text{nM}$ ethylenediaminetetraacetic acid (EDTA) and $2\ \mu\text{g/ml}$ F108 was used.

In Fig. 3, we present a sequence of images that illustrates the difference in the path of a tagged leukocyte from that of untagged red blood cells. The fluid layer is $15\ \mu\text{m}$ thick, the external field is $0.1\ \text{T}$, and the average flow speed is $110\ \mu\text{m/s}$, inferred from the red blood cells, which are not deflected. The path of the red blood cells can be seen from

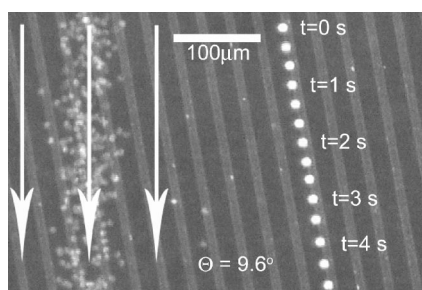


FIG. 3. Time lapse image showing a single tagged fluorescing leukocyte at different times tracking a magnetic stripe at an angle of 9.6° to the fluid velocity ($110 \mu\text{m/s}$) indicated by white arrows. Red blood cells on the left are from a single image. All cells entered the chip at the same point approximately 1.5 mm above the field of view.

the single image which comprises the background of Fig. 3. Superimposed is the fluorescent image of a single leukocyte at intervals of 0.33 s. It has become trapped over the magnetic stripe and follows it, diverging from the untagged cells.

Figure 4 shows histograms of multiple leukocyte separations under three different conditions. The lateral positions of the cells are measured with respect to the center of the red blood cell stream (defined as $x=0 \mu\text{m}$) after traveling 1.15 mm in the device. The magnetic stripes are tilted at $\theta=11^\circ$ to the fluid flow. In Fig. 4(a), the device has been demagnetized, no external magnetic field was applied, and the flow speed was $180 \mu\text{m/s}$. No separation occurred, and all cells followed the fluid flow direction to exit the camera's field of view at approximately $x=0 \mu\text{m}$. The width of the peak is identical to the width of the red blood cell stream.

In Fig. 4(b) an external magnetic field of 0.08 T was applied, and the flow speed was $240 \mu\text{m/s}$. There is a peak in the histogram at $x=220 \mu\text{m}$, representing 40% of the dis-

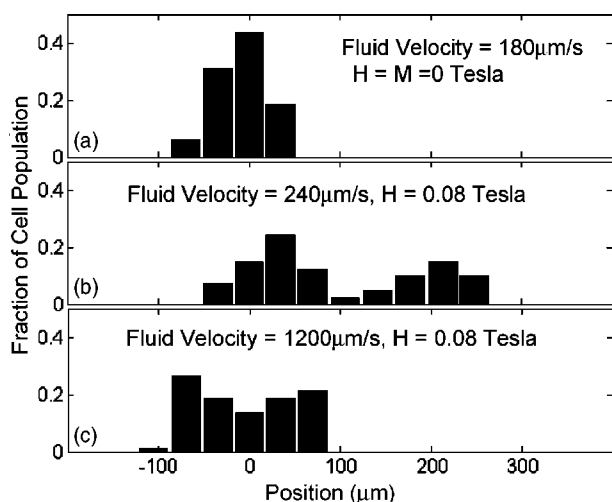


FIG. 4. Histograms comparing three different operating conditions. The positions of the cells are recorded at 1.15 mm into the device with the magnetic stripes at 11° to the fluid flow. The position of the undeflected red blood cell stream is defined as $x=0 \mu\text{m}$ (a) The external field is 0 T and the fluid velocity is $180 \mu\text{m/s}$. The width of the distribution is equal to the width of the red blood cell stream through the device. No separation has occurred. (b) The external field is 0.08 T, and the fluid velocity is $240 \mu\text{m/s}$. The peak at $220 \mu\text{m}$ represents a population of nucleated CD45+ that was separated from the red blood cells by traveling along magnetic stripes. The peak at $0 \mu\text{m}$ represents nucleated cells that were not separated. (c) The magnetic field is 0.08 T and the fluid velocity is $1200 \mu\text{m/s}$. No separation has occurred due to increased drag forces. The width of the distribution is equal to the width of the red blood cell stream.

tribution, which corresponds to cells becoming trapped and following magnetic stripes. Presumably the separation condition given in Eq. (3) has been met for these cells. We calculate the separation condition to be met for cells traveling slower than $240 \mu\text{m/s}$ for $\theta=11^\circ$, assuming 5000 beads on a $10 \mu\text{m}$ spherical cell on the bottom of the channel. The peak at approximately $x=30 \mu\text{m}$ contains 60% of all leukocytes; these have been deflected only slightly. The bimodal distribution may be caused by variations in the number of beads attached to cells.

In Fig. 4(c) the external magnetic field is still at 0.08 T, but the flow speed has been increased fivefold to $1200 \mu\text{m/s}$. In this case no separation has occurred and again the width of the distribution is equal to that of the red blood cell stream. The failure to separate occurs because the fluidic drag force which pushes the cells through each magnetic trap is now five times larger than in Fig. 4(b) while the magnetic force is unchanged.

We believe that with minor modifications such as increasing the thickness of the stripes and increasing the external field, the separation force can be increased by an order of magnitude, allowing for higher throughput and higher recovery.

In summary, we have presented a microfluidic implementation of a device which allows continuous cell by cell separation from a flow stream by selectively tagging with magnetic beads. The device uses microfabricated magnetic features to induce a lateral force on streaming tagged cells. The device has been used to separate leukocytes from whole blood and should be useful for integration into a microfluidic total analysis system (μTAS).

The authors greatly appreciate the many helpful conversations with B. Frazier, L. R. Huang, C. Prinz, S. Park and W. Ryu, and the previous work of M. Berger and M. Shaw. They also thank N. P. Ong and W. L. Lee for their assistance with the magnetometer. This work was supported by grants from DARPA (MDA972-00-1-0031), NIH (HG01506, E-21-F46-G1), NSF Nanobiology Technology Center (BSCECS9876771), the State of New Jersey (NJCS 99-100-082-2042-007), and the Office of Naval Research (ONR3396044). The authors acknowledge support from the Cornell University National Fabrication Center, where the chemical mechanical polishing and deep silicon etching were performed.

¹S. Miltenyi, W. Müller, W. Weichel, and A. Radbruch, *Cytometry* **11**, 231 (1990).

²A. B. Kantor, I. Gibbons, S. Miltenyi, and J. Schmitz, *Magnetic Cell Sorting with Colloidal Superparamagnetic Particles in Cell Separation Methods and Applications*, edited by D. Recktenwald and A. Radbruch (Marcel Dekker, New York, 1998), p. 153.

³J. J. Chalmers, M. Zborowski, L. Sun, and L. Moore, *Biotechnol. Prog.* **14**, 141 (1998).

⁴C. H. Ahn, M. G. Allen, W. Trimmer, Y. Jun, and S. Erramilli, *J. Microelectromech. Syst.* **5**, 1057 (1996).

⁵J. Choi, C. H. Ahn, S. Bhansali, and H. T. Henderson, *Sens. Actuators B* **68**, 34 (2000).

⁶N. Darnton, O. Bakajin, R. Huang, B. North, J. O. Tegenfeldt, E. C. Cox, J. Sturm, and R. H. Austin, *J. Phys.: Condens. Matter* **13**, 4891 (2001).

⁷A. Bikoue, G. Jonossy, and D. Barnett, *J. Immunol. Methods* **266**, 219 (2002).

⁸K. E. McCloskey, J. H. Chalmers, and M. Zborowski, *Anal. Chem.* **75**, 6868 (2003).

⁹T. McPherson, A. Kidane, I. Szeleifer, and K. Park, *Langmuir* **14**, 176 (1998).